Effect of Periodic Replacement of the Heteroatom on the Spectroscopic Properties of Indole and Benzofuran Derivatives

Atsuya Muranaka,*,†,‡ Shuji Yasuike,*,§,# Ching-Yuan Liu,†,# Jyoji Kurita,*,§ Naoki Kakusawa,§ Takashi Tsuchiya,§ Masako Okuda,‡ Nagao Kobayashi,*,‡ Yotaro Matsumoto,† Kengo Yoshida,† Daisuke Hashizume,† and Masanobu Uchiyama†

Advanced Elements Chemistry Laboratory, the Institute of Physical and Chemical Research (RIKEN), Wako-shi, Saitama 351-0198, Japan, Department of Chemistry, Graduate School of Science, Tohoku University, Aoba-ku, Sendai 980-8578, Japan, Department of Pharmaceutical Sciences, Hokuriku University, Ho-3, Kanagawa-machi, Kanazawa-shi, Ishikawa 920-1181, Japan, and Organization for Frontier Research in Pharmaceutical Sciences, Hokuriku University, Kanagawa-machi, Kanazawa 920-1181, Japan

Received: September 8, 2008; Revised Manuscript Received: October 27, 2008

The electronic structures of a homologous series of indole and benzofuran derivatives, in which the nitrogen or oxygen atom is replaced by group 15 and group 16 heavier heteroatoms, have been investigated by means of various spectroscopic techniques coupled with density functional calculations. It was found that the excitation energies of the group 16 benzoheteroles systematically shift to the red in the order of benzofuran (**6**), benzothiophene (**7**), benzoselenophene (**8**), and benzotellurophene (**9**). In contrast, the electronic absorption spectra of the group 15 benzoheteroles, 1-phenyl derivatives of indole (**1b**), phosphindole (**2b**), arsindole (**3b**), stibindole (**4b**), and bismuindole (**5b**), did not exhibit this type of spectral shift. X-ray analysis and density functional theory (DFT) studies revealed that **2b**−**5b** adopt a bent conformation both in the crystalline and in the solution phases. In contrast, planar structures were calculated for the group 16 heterocycles. Using the observed spectroscopic properties and time-dependent density functional theory (TDDFT) calculations, the electronic absorption spectra of the present heterocycles were assigned. A molecular orbital analysis was performed to rationalize the effect of replacement of the heteroatom on the electronic structures. The observed magnetic circular dichroism (MCD) sign patterns of these heterocycles are interpreted according to Michl's perimeter model.

Introduction

Benzo-fused five-membered heterocycles, such as indole (benzopyrrole, C_8H_6NH, **1a**), benzofuran (C_8H_6O, **6**), or benzothiophene (C_8H_6S, **7**), are among the most important domains of aromatic heterocyclic chemistry[1,2] and are of substantial utility in pharmaceutical, agrochemical, and material sciences[3−16] as platforms in pigments, biogenic amino acids or proteins, and alkaloids, as modular components in drugs, and as uniquely effective substituents in organic synthesis. Nitrogen and oxygen are neighbors in the periodic table, and the similarity in their basic properties has been well documented by experimental chemists. For example, indole (**1a**) and benzofuran (**6**) exhibit significantly similar (planar) structures, electronic properties, and reactivities and selectivities in organic synthesis, and hence these heterocycles and their derivatives have long been regarded as belonging to the same category. However, these similarities might also be essentially superficial, since they are in different groups (groups 15 and 16). Thus, it is of interest to carry out a systematic investigation and to clarify the similarities and differences between a homologous series of indole and benzofuran derivatives.

From a theoretical point of view, these aromatic heterocycles can be derived from an indenide anion ($C_9H_7^-$) by the introduction of a heteroatom which contributes two electrons to the conjugated system.[17,18] In this respect, benzo-fused five-membered heterocycles (heteroles) containing a heavier main group atom other than nitrogen, oxygen, or sulfur have also attracted considerable interest in terms of their syntheses, structures, and physicochemical properties.[19−22] In 1993, one of our groups established a simple synthetic route to a variety of C-unsubstituted 1-benzoheteroles containing group 15 (P, As, Sb, and Bi) and group 16 (Se and Te) elements from phenyl(trimethylsilyl)acetylene via a common dilithiostyrene intermediate.[23,24] Although one might expect that the heavier main group element in the aromatic heterocycles would significantly affect their structural and optical properties, to date very little is known about the effect of the heteroatom on their physicochemical properties. We believe that an in-depth understanding of the electronic structures of indole and isoelectronic heterocyclic systems would play an important role in the design of new organic materials and drugs containing these molecular frameworks.

In the present research, the physicochemical natures of indole (C_8H_6NH), phosphindole (1-benzophosphole: C_8H_6PH), arsindole (1-benzarsole: C_8H_6AsH), stibindole (1-benzostibole: C_8H_6SbH), bismuindole (1-benzobismole: C_8H_6BiH), benzofuran (C_8H_6O), benzothiophene (C_8H_6S), benzoselenophene (C_8H_6Se), and benzotellurophene (C_8H_6Te) (**1**−**9**, see Chart 1) have been comprehensively investigated by electronic absorption, circular dichroism (CD), and magnetic circular dichroism (MCD)

* To whom correspondence should be addressed. E-mail: atsuya-muranaka@riken.jp (A.M.), s-yasuike@hokuriku-u.ac.jp (S.Y.), j-kurita@hokuriku-u.ac.jp (J.K.), nagaok@mail.tains.tohoku.ac.jp (N.K.).
† RIKEN.
‡ Tohoku University.
§ Hokuriku University.
# Organization for Frontier Research.

10.1021/jp8079843 CCC: $40.75
Published on Web 12/18/2008

CHART 1: Structures of Indole and Benzofuran Derivatives in this Study

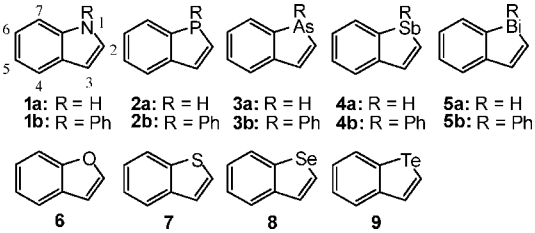

spectroscopies and X-ray diffraction. Since the parent phosphindole (**2a**), arsindole (**3a**), stibindole (**4a**), and bismuindole (**5a**) are known to be unstable, we have investigated the spectroscopic properties of their 1-phenyl derivatives (**1b**−**5b**). To clarify their structural and electronic features and to make band assignments of the present systems in solution, density functional theory (DFT) and time-dependent DFT calculations have been carried out. A large difference in the structural and electronic characteristics was seen between group 15 and group 16 benzoheteroles. On the basis of these observations, the origin of the spectroscopic properties of the various heterocycles was successfully explained by applying the perimeter model provided by Souto et al., who predicted the effect of the MCD sign pattern for the L transitions on the replacement of the heteroatom in indole systems.[17]

Computational Details

All calculations were performed with a Gaussian 03 (G03) program package[25] using the hybrid density functional method based on Becke-3 parameter exchange functional and the Lee−Yang−Parr nonlocal correlation functional (B3LYP). 6−31+G* basis sets were used on carbon and hydrogen atoms, while a 3−21G** basis set was used for the heteroatom. Geometry optimization and time-dependent DFT calculations were performed at the same level. Since the molecules in this study contain heavy main group atoms, we also carried out geometry optimization and time-dependent density functional theory (TDDFT) calculations using the Los Alamos effective-core potential (ECP) LanL2DZ basis set,[26−28] and we investigated the effect of the basis sets on the calculated values. The phenyl plane of 1-phenyl indole was set to be perpendicular to the indole skeleton for the calculations of TDDFT and molecular orbital (MO) analysis to compare the results of the other heavier benzoheteroles with perpendicular orientation. Geometry optimization and time-dependent DFT calculations of 1-phenyl benzoheteroles with planar structures were carried out by imposing C_s symmetry. Solvent effect was not taken into account in the calculations since such an effect was not observed experimentally.

Results

1. λ_{max} of Group 15 and Group 16 Benzoheteroles. 1-Phenyl indole (**1b**) was prepared using the copper-catalyzed N-arylation method described by Chang et al.[29] Group 15 and group 16 benzoheteroles with heavier heteroatoms (**2b**−**5b** and **7**−**9**) were synthesized from phenyl(trimethylsilyl)acetylene (**10**) in four steps via a common key 1,4-dilithiostyrene intermediate (**12**).[23,24] The benzoheteroles prepared in the present study exhibit characteristic UV spectra depending on their groups. To date, the spectroscopic properties and electronic structures of indole have been intensively investigated.[30−37] According to the Platt nomenclature,[38] the electronic transitions in the indole and isoelectronic heterocyclic chromophores are labeled, from the long-wavelength side, as L_1, L_2, B_1, and B_2 bands. These are $\pi \rightarrow \pi^*$ transitions. The two L transitions of indoles usually give strongly overlapping bands of medium intensity in the range of 250−300 nm, and the B_1 and B_2 transitions give more intense bands at ca. 220 and ca. 200 nm, respectively. Figure 1 shows the L band UV spectra of the series of 1-phenyl indole derivatives (**1b**−**5b**) and benzofuran derivatives (**6**−**9**). Table 1 summarizes the λ_{max} of these molecules. As is clearly seen, the λ_{max} of the group 16 heterocycles systematically shifts to the red (by ca. 10 nm) with increasing size of the heteroatom, while the group 15 heterocycles do not exhibit a systematic spectral shift.

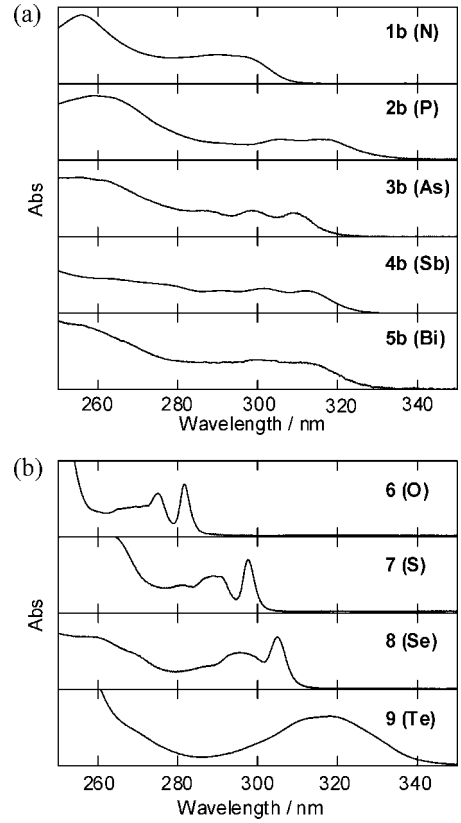

Figure 1. Spectral changes for the lowest-energy UV absorption band for a series of group 15 (a) and group 16 (b) benzoheterole derivatives measured in methanol at room temperature.

TABLE 1: Spectral Data for the Lowest-Energy Absorption Bands of Benzoheterole Derivatives (in Methanol)

compound	λ_{max}/nm	10^{-4} ν_{max}/cm^{-1}	10^{-3} ϵ/M^{-1} cm^{-1}	atomic radius[a]/Å
1b (N)	290	3.45	8.2	0.75
2b (P)	315	3.17	4.1	1.06
3b (As)	309	3.24	2.3	1.20
4b (Sb)	313	3.19	4.2	1.40
5b (Bi)	312	3.21	3.5	1.46
6 (O)	282	3.55	4.8	0.73
7 (S)	298	3.36	8.1	1.02
8 (Se)	305	3.28	5.5	1.16
9 (Te)	317	3.15	5.8	1.36

[a] Data from ref 39.

Figure 2 shows plots of atomic radius[39] versus the wavenumber for the lowest-energy transition for either series of compounds. Interestingly, the excitation wavenumber in the group 16 heterocycles varies in proportion to their atomic radius. This type of relationship is not seen in the group 15 derivatives.

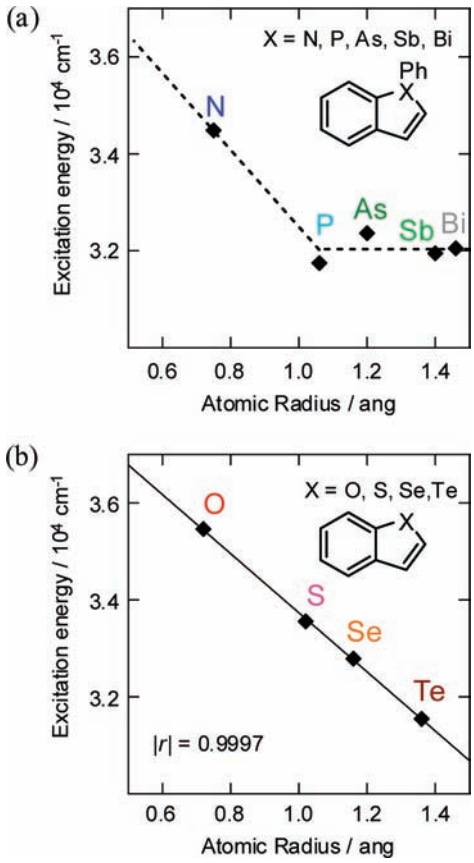

Figure 2. Plots of atomic radius (Å)[39] vs excitation energy (cm^{-1}) for the lowest-energy transition for a series of benzoheterole derivatives. (a) Group 15 derivatives. (b) Group 16 derivatives. The straight line was drawn using the least-squares method.

It appears that the electronic structures of the heavier heterocycles (**2b**−**5b**) are considerably different from that of the indole (**1b**). In the following sections, the difference in the spectroscopic properties between the group 15 and the group 16 heterocycles is investigated in detail.

2. Group 15 Heterocycles. ***2.1. Solid-State Structures.*** According to the X-ray crystal structure analysis of 1-phenyl phosphindole (**2b**), the phosphindole skeleton is planar and the P atom is tetrahedrally coordinated.[40] This is in contrast to the planar coordination of the N-atom in the phenyl indole derivatives.[41,42] To further understand the solid-state structures of the group 15 heterocycles, we have carried out X-ray analysis of 1-phenyl arsindole (**3b**). Single crystals suitable for the X-ray analysis were obtained from a methanol solution of **3b** by solvent evaporation. The molecular structure of **3b** is shown in Figure 3. The atomic coordinates, selected bond distances, and angles are summarized in the Supporting Information (Table S1). It is evident from the figure that the As atom in **3b** adopts a tetrahedrally coordinated geometry. The parent arsindole skeleton is almost planar, and the bond distance between C1 and C2 (1.330(3) Å) was within the range typical for C═C bond distances. These characteristics are close to those revealed by the structure of 1-phenyl phosphindole (**2b**).

2.2. Solution Structure of Stibindole. The results for the X-ray analyses imply that 1-phenyl benzoheteroles with heavier heteroatoms become an intrinsically chiral molecule. In the case of 1-phenyl stibindole (**4b**), its chiral structure has been confirmed from the fact that the enantiomers can be obtained using the optically active ortho-palladated benzylamine derivative via their diastereomeric complexes.[43] To determine the

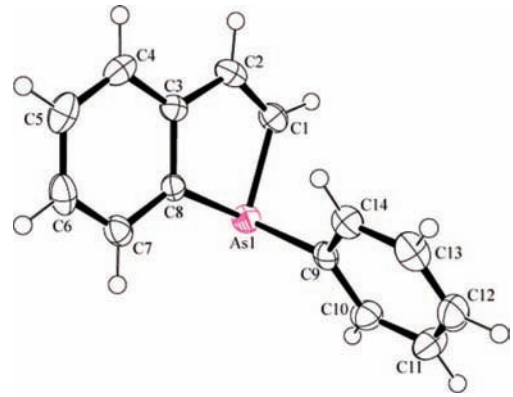

Figure 3. An ORTEP drawing of 1-phenyl arsindole (**3b**). Displacement ellipsoids are drawn at the 50% probability level.

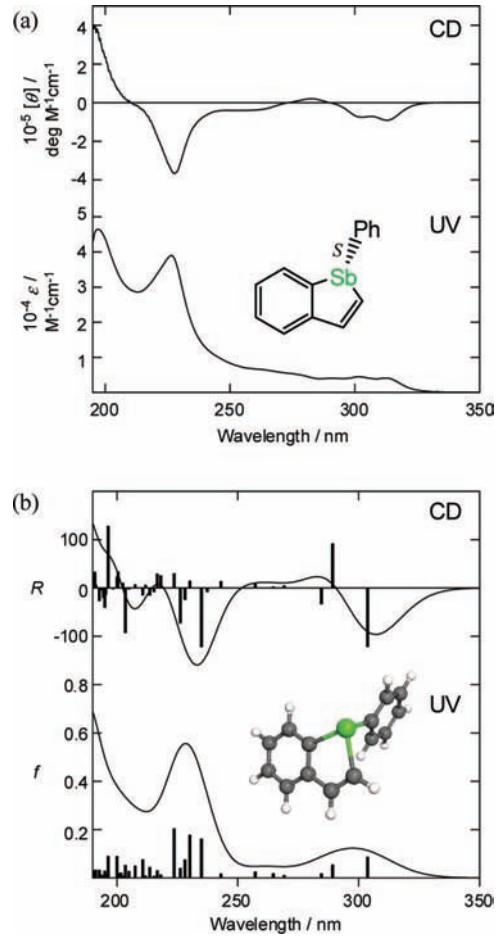

Figure 4. (a) Experimental UV and CD spectra of (*S*)-1-phenyl stibindole ((*S*)-**4b**) measured in methanol at room temperature. (b) Calculated UV and CD spectra of (*S*)-**4b** obtained using the TDDFT method. Rotational strengths are given in cgs (10^{-40} erg esu cm/Gauss). Gaussian bands with a half-bandwidth of 3000 cm^{-1} were used to simulate the spectra. The inset shows the optimized geometry of (*S*)-**4b** (B3LYP/6−31+G* (3−21G** for Sb)).

chiral structure of (*S*)-**4b** in solution, we measured its experimental CD spectrum and calculated its theoretical CD spectrum using the TDDFT method. As shown in Figure 4a, (*S*)-**4b** exhibited an intensely negative CD signal corresponding to the 230 nm absorption band. With respect to the longer wavelength region, a negative CD pattern was observed beyond 300 nm, while a weakly positive CD band was seen at around 290 nm. The heteroatom in the optimized structure of (*S*)-**4b** adopts an essentially tetrahedral arrangement similar to those seen in the

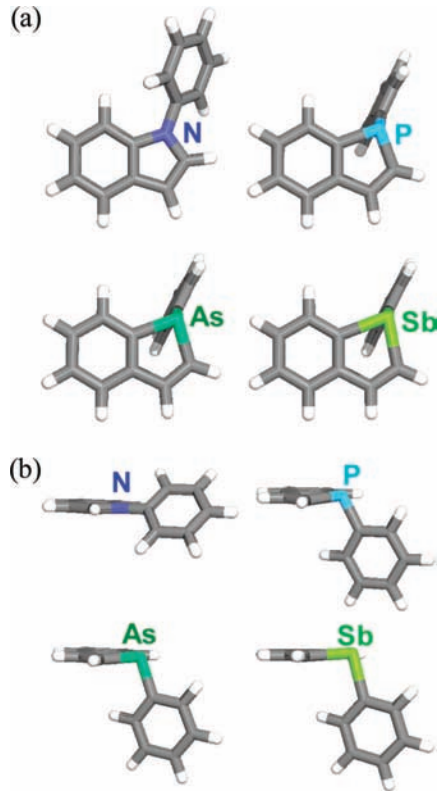

Figure 5. Optimized structures of the group 15 heterocycles (B3LYP/6−31+G*(3−21G** for the heteroatom). (a) Top view. (b) Side view.

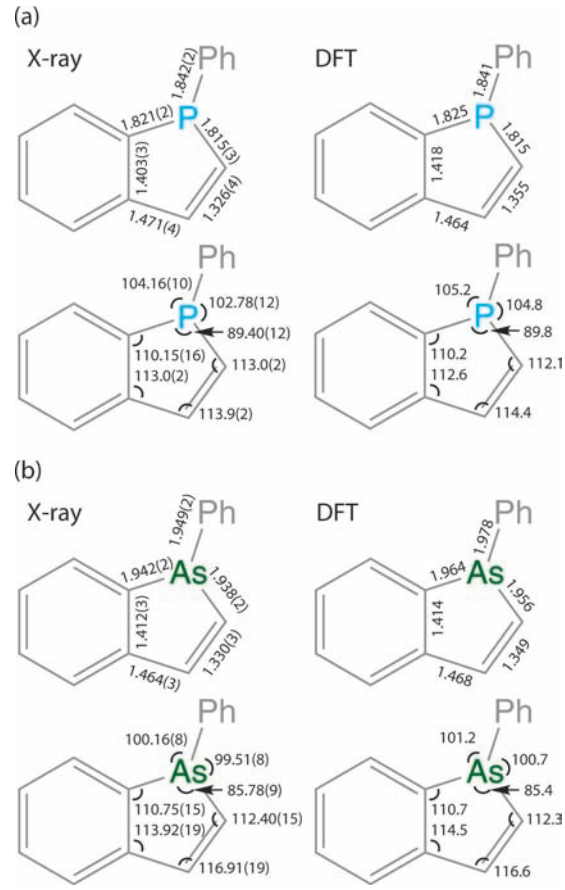

Figure 6. Experimental and optimized bond distances (Å) and angles (deg) for 1-phenyl-1-benzoheteroles. (a) 1-Phenyl phosphindole (**2b**). The data is from ref 40. (b) 1-Phenyl arsindole (**3b**). Geometry optimizations were carried out at the level of B3LYP/6−31+G* (3−21G** for the heteroatom).

crystal structures of **2b** and **3b**. The calculated absorption and CD spectra for the optimized structure of (*S*)-**4b** agreed well with the experimental spectra (Figure 4b). We can therefore conclude that 1-phenyl stibindole exists in a nonplanar form in methanol solution.

2.3. Calculated Structures. Figure 5 presents the DFT-optimized geometries of the 1-phenyl indole derivatives (**1b**−**4b**). As is clearly seen, all the π frameworks are virtually planar. The calculated bond distances between the 2 and 3 positions (see Chart 1) in the phosphindole (**2b**), arsindole (**3b**), and stibindole (**4b**) were 1.355, 1.349, and 1.349 Å, respectively, which are slightly shorter than that of the indole (**1b**, 1.369 Å). The N atom in **1b** has a flat coordination structure, while the other heterocycles adopt a bent conformation, which strongly supported the experimental results of X-ray diffraction studies. The calculated bond distances and angles of 1-phenyl phosphindole (**2b**) and 1-phenyl arsindole (**3b**) are in excellent agreement with their experimentally determined solid-state structures (Figure 6). The bent conformations of these heterocycles were also predicted using the LanL2DZ basis sets. The P, As, and Sb atoms in the optimized geometries of the heterocycles without the phenyl substituent (**2a**−**4a**) were also approximately tetrahedral[44] suggesting that the tetrahedral coordination arises from the intrinsic properties of the heteroatoms.

2.4. UV and MCD Spectra. Magnetic circular dichroism (MCD) spectroscopy is a useful tool for investigating the electronic structures and band assignments of aromatic molecules since the MCD effect in some aromatic molecules has a relatively simple physical origin.[45−47] Studies on the MCD spectra of indoles, benzofuran, and benzothiophene have been reported previously by several groups.[17,18,48−50] According to the previous investigations of indole, two L transitions can be resolved in the MCD spectra as the L_1 and L_2 transitions are polarized in different directions and as the transitions can couple in a magnetic field giving rise to differently signed MCD signals (two Faraday *B* terms). We have therefore measured the MCD spectra of the series of benzoheteroles with heavier heteroatoms.

Figure 7 shows the UV and MCD spectra of the 1-phenyl indole derivatives (**1b**−**5b**). All these heterocycles exhibit broad absorption bands in the UV region. An intense absorption peak, which can be assigned as the B_1 band, is seen at around 210−230 nm for each heterocycle. The lowest-energy absorption band of the indole (**1b**) lies at ca. 290 nm, while those of the other heterocycles are seen in the 300−320 nm region. A broad absorption band was observed at around 260 nm for all the derivatives. The heterocyclic compounds exhibited a +, − MCD sign pattern, in ascending energy term, corresponding to the absorption bands in the 270−320 nm region. These signals can be assigned to coupled Faraday *B* terms arising from the magnetically induced mixing of two L transitions.[51,52] Thus, we can conclude that the L_2 band of the group 15 benzoheteroles is located at ca. 280 nm.

To make band assignments, time-dependent density functional theory (TDDFT) calculations were performed for all the optimized geometries.[53−55] The calculated spectra of **1b**−**4b** are also shown in Figure 7. The lowest-energy transition of 1-phenyl indole (**1b**) was calculated to lie at 266 nm, while those of the P, As, and Sb derivatives were at 295, 292, and 304 nm, respectively. Although the calculations somewhat overestimate the excitation energies, the appearances of the calculated spectra are in close agreement with the experimental spectral patterns. A plot of the averaged carbon−heteroatom distance (Å) versus

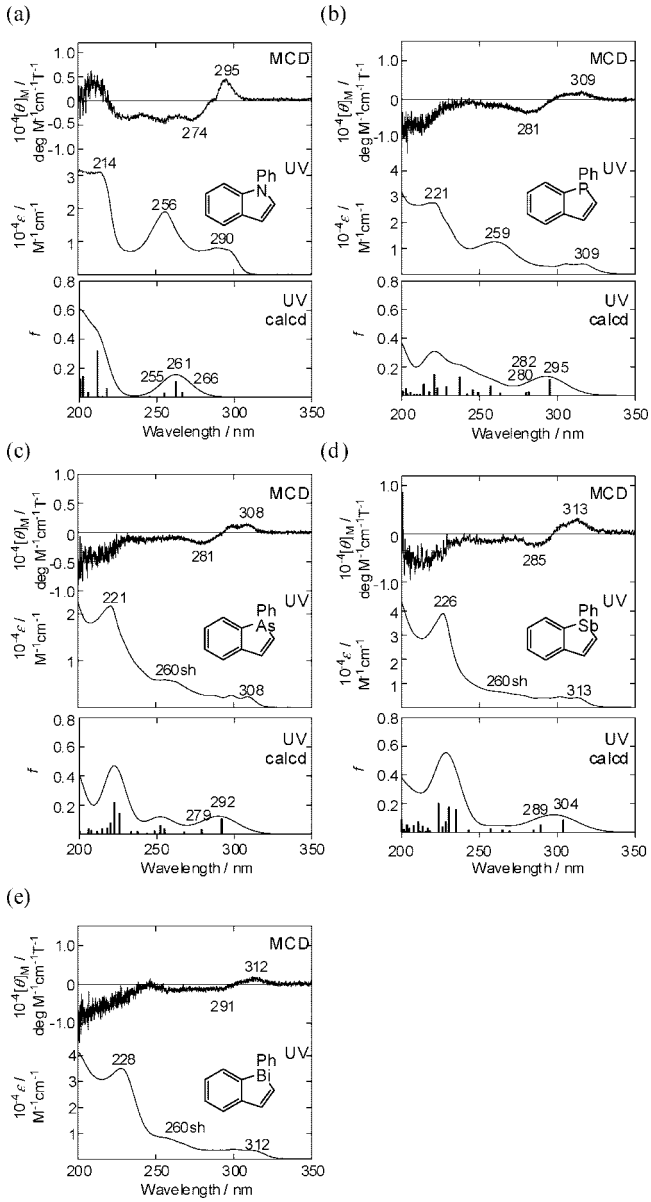

Figure 7. Experimental MCD and UV spectra of a series of 1-phenyl indole derivatives measured in methanol at room temperature. Calculated electronic absorption spectra of 1-phenyl indole derivatives (**1b**−**4b**) obtained using the TDDFT method (B3LYP/6−31+G* (3−21G** for the heteroatom)) are shown in the bottom of the experimental spectra. Gaussian bands with a half-bandwidth of 3000 cm^{-1} were used to simulate the spectra.

excitation energy for the lowest-energy transition (cm^{-1}) gave a similar pattern to the experimental results. Transition energies, oscillator strengths, and compositions for the two L bands are summarized in the Supporting Information (Table S2). In all the molecules, the direction of the transition moment for the L_1 transition is different from that of the L_2 transition, which is in agreement with the experimental observation that two differently signed MCD signals were observed for the long-wavelength region. The lowest and second lowest energy transitions of the arsindole and stibindole derivatives were ascribed to the L_1 and L_2 transitions, although a charge-transfer transition from the benzoheterole skeleton to the phenyl substituent contributes to the L transitions of the indole and phosphindole. The weakly positive CD band observed for (*S*)-**4b** (Figure 4) is therefore associated with the L_2 transition. The TDDFT calculations using the LanL2DZ basis sets gave the same spectral properties as

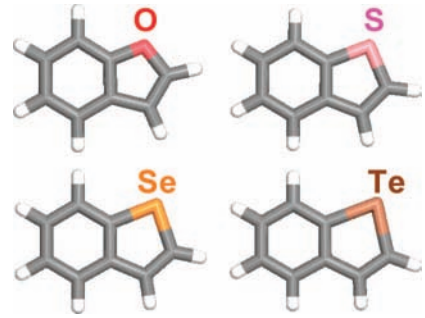

Figure 8. Optimized structures of the group 16 heterocycles (B3LYP/6−31+G* (3−21G** for the heteroatom)).

the 6−31+G* basis sets (see Supporting Information). We have also calculated the excited states of the group 15 benzoheteroles without phenyl substituents (**1a**−**4a**) (Figure S1). In **1a**−**4a**, the lowest and second lowest energy transitions were ascribed to the L_1 and L_2 transitions.

Overall, from these experimental and computational results, it is now clear that the unique spectroscopic properties observed for the benzoheteroles containing a heavier heteroatom (P, As, Sb, or Bi) arise from their nonplanar structures. The planar indole has considerably different properties compared with those of the heavier benzoheteroles. This can be confirmed by performing theoretical calculations on the forced planar structures of the P, As, and Sb derivatives: the calculated excitation energy for the lowest-energy transitions shifts to red in proportion to the size of heteroatom as is the case with the group 16 derivatives (see Figure S2).

3. Group 16 Heterocycles. ***3.1. Calculated Structures.*** The DFT-optimized geometries of the group 16 benzoheteroles are presented in Figure 8. It is well-known that benzofuran (**6**) and benzothiophene (**7**) have a planar structure.[56−58] The present computational results demonstrate that benzoselenophene (**8**) and benzotellurophene (**9**) are also planar. The calculated bond distances between the 2- and 3-positions (see Chart 1) in **7**, **8**, and **9** are 1.362, 1.357, and 1.356 Å, respectively, which are almost the same as that computed for benzofuran (**6**, 1.358 Å). This is in contrast to the results of the group 15 systems. Geometry optimizations using the LanL2DZ basis sets also predicted planar structures for the group 16 systems.

3.2. UV, MCD, and CD Spectra. The UV and MCD spectra of the benzofuran derivatives (**6**−**9**) in methanol are shown in the Supporting Information (Figure 9). Benzofuran (**6**) has two absorption bands at 282 and 243 nm, which have been assigned to two L transitions.[17,48] The MCD sign sequence for the L bands is +, −, in ascending energy, which is associated with the differently polarized electronic transitions. The UV spectrum of benzothiophene (**7**) shifts to the red compared with that of **6**: the two L transitions are observed at 298 and 256 nm, and the B_1 transition is observed at 225 nm.[17,48] The MCD pattern for the L bands is the same as that of **6**. Both the absorption and MCD spectra of benzoselenophene (**8**) showed further red-shifted absorption bands. The L_1, L_2, and B_1 transitions of **8** can be assigned to the absorption bands at 305, 260 (sh), and 235 nm, and their MCD sign sequence is +, −, −. In the case of benzotellurophene (**9**), the UV spectrum showed broad, red-shifted absorption bands across the whole UV region. Although several vibronic bands are clearly seen in **6**, **7**, and **8**, the vibronic bands are not resolved in **9**. The 252 nm band is presumably the B_1 transition. The MCD sign corresponding to the lowest-energy absorption band of **9** was opposite that of the other group 16 heterocycles: a −, + sign sequence was observed for the 270−310 nm region.

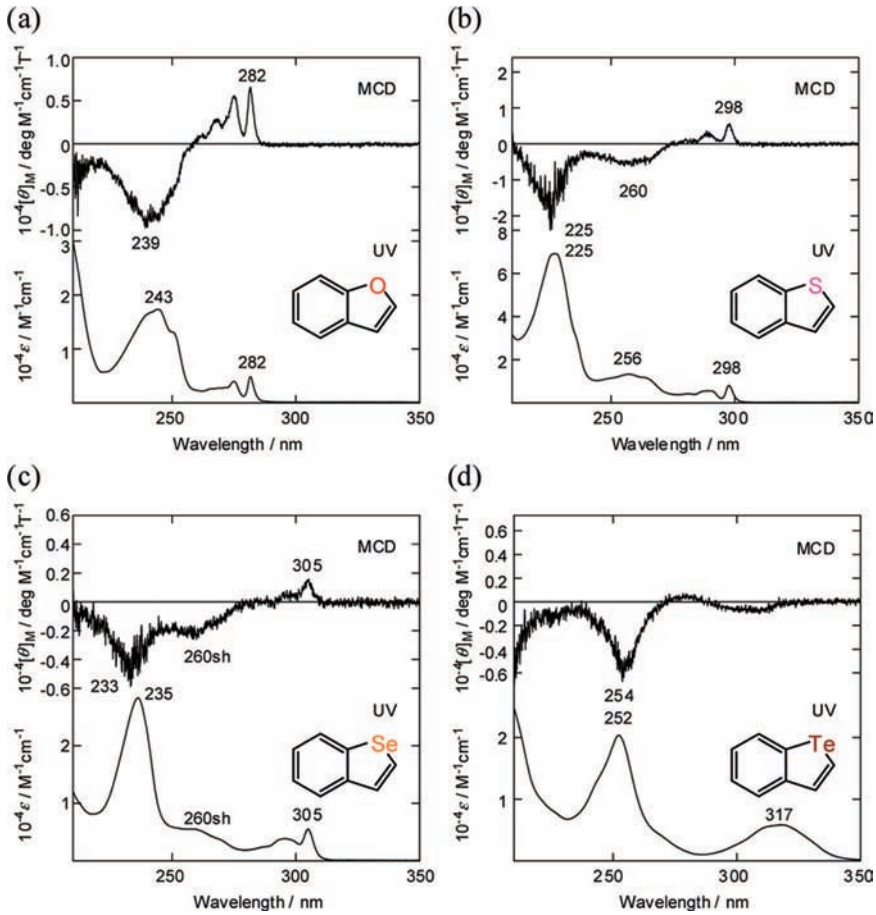

Figure 9. Experimental MCD and UV spectra of a series of benzofuran derivatives (**6**−**9**) measured in methanol at room temperature.

To gain an insight into the polarization directions of the group 16 heterocycles, the induced CD spectra as well as the MCD spectra were measured by complexation with β-cyclodextrin (β-CDx) in water. The induced CD of β-CDx complexes with achiral organic aromatic compounds, such as naphthalene and pyrene derivatives, is useful for determining the relative orientations of electric transition dipole moments for the organic aromatic compounds.[59] The structures of these inclusion complexes can be regarded as being based upon axial inclusion of the guest molecule such that its long axis is parallel to the axis of the β-CDx cavity. The result is that the long- and short-axis polarized transitions may give rise to positive and negative induced CD signals, respectively.

Figure 10 shows the CD, MCD, and UV spectra of the β-CDx complexes of benzofuran derivatives **6**−**9**. The inclusion complexes were prepared by mixing the corresponding benzofuran derivative with an excess amount of β-CDx in aqueous solution. Since the UV and MCD spectral pattern of the complexes appears to be identical to those of the heterocycles measured in methanol, it is reasonable to assume that β-CDx does not significantly affect the electronic structures of the benzoheteroles. In the case of benzothiophene (**7**), benzoselenophene (**8**), and benzotellurophene (**9**), a positive induced CD signal was observed corresponding to the B_1 bands, while the induced CD for benzofuran (**6**) had almost no intensity. The results indicate the predominance of long-axis-polarized electronic transitions for the B_1 transitions.

Figure 10 also presents the calculated absorption spectra of **6**−**9**. Transition energies, oscillator strengths, and compositions for the L_1, L_2, and B_1 transitions are summarized in the Supporting Information (Table S3). The calculations predicted that the transition energies for the lowest-energy transition (L_1 transition) of benzofuran (**6**), benzothiophene (**7**), benzoselenophene (**8**), and benzotellurophene (**9**) are 249, 267, 278, and 303 nm, respectively, reproducing the systematic red-shift observed experimentally. Akin to the results obtained for the group 15 derivatives, the excitation energies are overestimated to some extent. A linear relationship between the averaged carbon−heteroatom distance (Å) and the excitation energy for the lowest-energy transition (cm^{-1}) was obtained, which reproduces the experimental results (see Supporting Information (Figure S2)). The oscillator strength of the L_2 transitions was calculated to decrease as the size of the heteroatom increased. This trend is clearly in agreement with experimental observation (see Figures 9 and 10). From the observed and calculated spectra of benzotellurophene (**9**), the absorption band at around 270 nm can be associated with the L_2 transition. The calculated 208, 224, 232, and 245 nm transitions were assigned to the B_1 bands of **6**, **7**, **8**, and **9**, respectively. The arrow in Figure 10e shows the direction of electric transition dipole moment for the B_1 transition of the heterocycles. Since the polarization directions of these transitions are nearly longitudinal, positive induced CD signals are predicted theoretically.[59] This is in line with our experimental observations. The TDDFT calculations using the LanL2DZ basis sets gave the same spectral properties as the 6−31+G* basis sets (see Supporting Information (Figure S3)).

Discussion

MO Analysis. To enhance our understanding of the nature of the benzoheteroles studied, an MO analysis was carried out. Figure 11a shows the energy levels of four key frontier π-orbitals and their contour plots for the benzoheteroles.

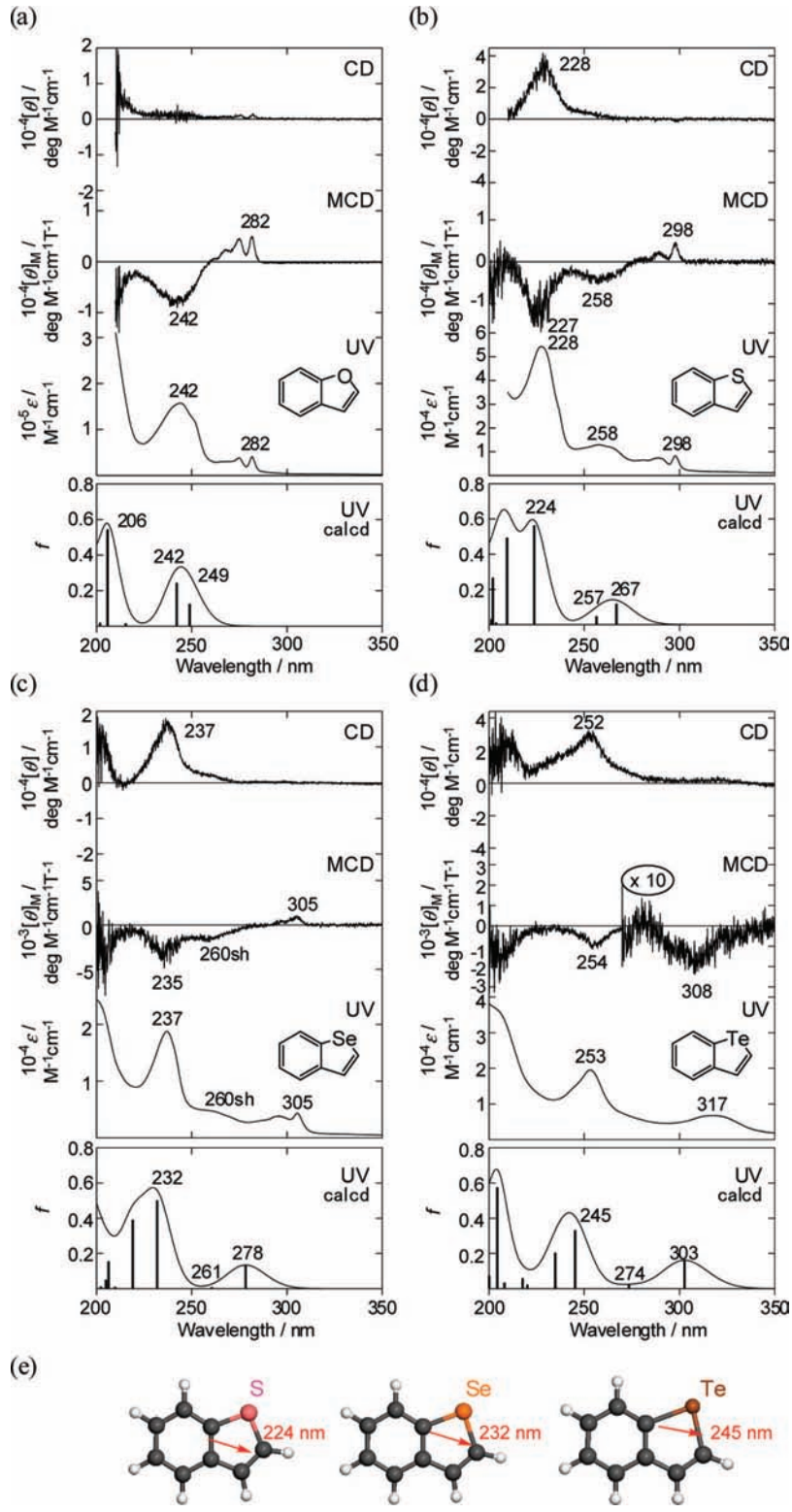

Figure 10. Experimental CD (top), MCD (middle), and UV (bottom) spectra of the β-cyclodextrin complexes of benzofuran (**6**, a), benzothiophene (**7**, b), benzoselenophene (**8**, c), and benzotellurophene (**9**, d) in aqueous solution at room temperature. Calculated electronic absorption spectra of benzofuran derivatives (**6**−**9**) obtained using the TDDFT method (B3LYP/6−31+G* (3−21G** for the heteroatom)) are shown in the bottom of the experimental spectra. Gaussian bands with a half-bandwidth of 3000 cm^{-1} were used to simulate the spectra. (e) Direction of electric dipole moment for the B_1 band in each of **7**, **8**, and **9**.

Excitations of electrons between these orbitals contribute to the L and B transitions of the present system. In the case of the group 15 derivatives, the energy levels of the indole (**1b**) are higher than the orbitals of the other heterocycles, but the orbital energies and the contour plots of 1-phenyl phosphindole (**2b**), arsindole (**3b**), and stibindole (**4b**) are very similar to one another. This may originate from the bent conformation of **2b**−**4b**. Because of the presence of the phenyl substituent, energy levels arising from the phenyl substituent are present in the unoccupied MOs. From these results, one can confirm that the characteristic energy levels of the frontier π-orbitals are related to the experimental result that the excitation energy of

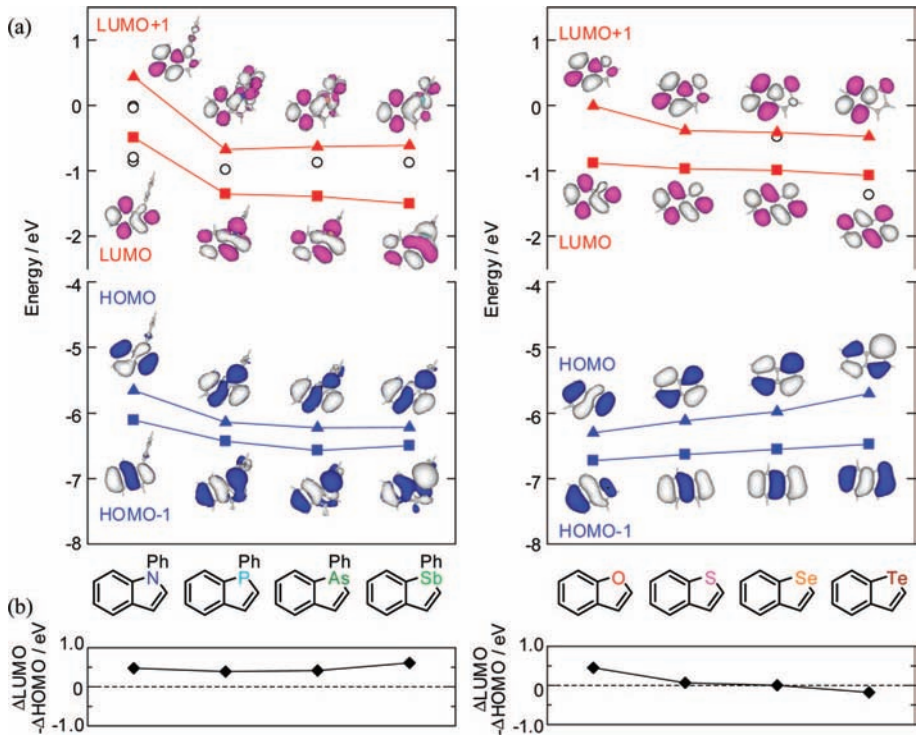

Figure 11. (a) Energy levels of four key molecular orbitals and their contour plots for group 15 and group 16 heterocycles. The white circles indicate the energy levels that are not associated with the π orbitals of the skeleton. (b) Energy difference between the ΔHOMO and ΔLUMO. The values were obtained from the B3LYP/6−31+G* (3−21G** for the heteroatom) calculations.

the indole (**1b**) is considerably different from those of the heavier heterocyclic systems (**2b**−**5b**). The contour plots of the π orbitals of the group 15 benzoheteroles without phenyl substituents (**1a**−**4a**) are almost identical to those of **1b**−**4b** (see Supporting Information (Figure S4)).

Interestingly, we found that the HOMO−LUMO gap of the group 16 derivatives decreases with increasing size of the heteroatom. The systematic change in the HOMO−LUMO gap should be associated with the linear relationship between the atomic radius and excitation energy. The appearances of the contour plots of the HOMOs and HOMO−1s of these heterocycles with heavier heteroatoms (**7**−**9**) are quite similar to those of naphthalene. Although the actual LUMO of benzotellurophene (**9**) is a heteroatom-centered orbital, the MO does not contribute to the L or B transitions.

The calculations using the LanL2DZ basis sets of the group 15 and group 16 benzoheteroles predict the energy levels and contour plots for the group 15 and group 16 benzoheteroles that are similar to those calculated using the 6−31+G* basis sets (see Supporting Information (Figure S5)).

Michl's Perimeter Model. The basic interpretation of the MCD spectrum of indole and its analogues was put forward originally by Michl, who interpreted the MCD signals for L and B bands using the four frontier molecular orbitals.[17,47] In his perimeter model, the MCD signs for the L transitions are derived mainly from μ^+ contributions. The definition of the magnetic moment μ^+ has been described in ref 45. Two parameters, ΔHOMO and ΔLUMO, are used to estimate their MCD sign and magnitude. ΔHOMO and ΔLUMO represent the differences between the two highest occupied and the two lowest virtual MOs, respectively. From a theoretical point of view, ΔHOMO reflects the hindrance to the circulation of the positive hole which the promoted electron leaves behind in the originally degenerate HOMO of a perimeter, and ΔLUMO reflects the hindrance to the circulation of the excited negative

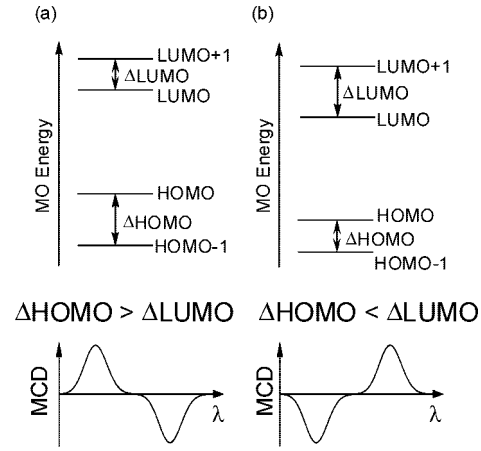

Figure 12. Relationship between the four frontier orbitals and the predicted MCD signs for the two L bands. (a) ΔHOMO > ΔLUMO. (b) ΔHOMO < ΔLUMO.

electron in the originally degenerate LUMO of a perimeter. If ΔHOMO = ΔLUMO, the μ^+ contribution vanishes; if ΔHOMO > ΔLUMO, electron circulation dominates; the predicted MCD signs for the two L transitions are −, + in order of increasing energy. If ΔHOMO < ΔLUMO, hole circulation dominates, and the predicted MCD signs for the two L transitions are the opposite. Figure 12 illustrates the relationship between the four frontier orbitals and the predicted MCD pattern.

In 1980, Souto et al. predicted that ΔHOMO < ΔLUMO for the heterocyclic molecules obtained by replacement of CH^- in an indenide anion by N^-, NH, NR, O, S, Se, and similar heteroatoms which hold an electron pair more tightly than CH^-.[17] Figure 11b shows the energy differences between the ΔHOMO and ΔLUMO. In the case of the group 15 molecules, ΔHOMO < ΔLUMO was calculated for all the compounds. This agrees well with the observed MCD spectra showing a +,

− sign sequence for the two L transitions. A ΔHOMO < ΔLUMO relationship was also predicted for the group 15 benzoheteroles without phenyl substituents (**1a**−**4a**) (Figure S4). On the other hand, we found that the ΔLUMO − ΔHOMO value for the benzofuran derivatives decreases with increasing size of the heteroatom (Figure 11 right and Figure S5 right). This should be related to the destabilization of the HOMO for the heterocycles with heavier heteroatoms. ΔHOMO > ΔLUMO was calculated for benzotellurophene (**9**) thus leading to the prediction of a −, + sign sequence for the two L transitions. The spectra shown in Figures 9 and 10 demonstrate that this MCD sign inversion actually occurs. In addition, according to the perimeter model, the L_2 band should have zero intensity if ΔHOMO and ΔLUMO are exactly equal. In the group 16 system, both the experimental (Figure 10) and TDDFT results (Table S4) indicate that the L_2 intensity decreases as the size of the heteroatom increases. Since the size of ΔHOMO of the heavier heterocycles reaches the size of ΔLUMO, all these results are in accordance with the perimeter model. Calculations using LanL2DZ basis sets also predict this relationship (see Supporting Information (Figure S5 right)).

As a consequence, the simple consideration of frontier MOs permits qualitative interpretations in the two L bands of the MCD spectra of the benzoheteroles. The group 15 benzoheteroles (**1b**−**5b**) can be classified as "negative-hard" chromophores, whose MCD sign pattern is difficult to change through replacement of the heteroatom. On the other hand, the group 16 derivatives (**6**−**9**) should be "soft" chromophores, whose MCD sign will change as a result of perturbation of the heteroatom. Souto et al. reported that the difference between ΔHOMO and ΔLUMO in indole can be reversed by a strong perturbation because the difference is relatively small.[17] To our knowledge, the MCD of benzotellurophene (**9**) is the first example of indole-type molecules with ΔHOMO > ΔLUMO relationship.

Conclusions

We have comprehensively investigated the physicochemical natures of a group of aromatic heterocycles derived from an indenide anion to obtain a clear-cut picture of how the heteroatom affects their spectroscopic properties and thereby also to design suitable heterocyclic molecules for potential applications. The main result is that replacement of the group 16 heteroatom causes a considerable spectral shift depending on the size of the heteroatom. We found that the excitation energy for the lowest-energy transitions in the benzofuran derivatives shifts to red in proportion to the size of the heteroatom. However, in the case of group 15 heterocycles, the spectroscopic properties do not change significantly even if the heteroatom is replaced by a heavier element. The CD and MCD techniques coupled with TDDFT calculations can afford definitive band assignments for these heterocyclic systems. The two L bands of the heterocycles were unambiguously identified using MCD spectroscopy. The B bands in the group 16 benzoheteroles were detected by the induced CD signals of their β-cyclodextrin complexes. The observed MCD sign sequence as well as the UV spectral features were successfully explained by considering the four frontier MOs. The systematic red-shift observed for the group 16 derivatives is shown to arise from destabilization of the HOMO of benzoheteroles as heavier heteroatoms are introduced. We have verified Michl's prediction for the MCD signs of the benzoheteroles.

The present study demonstrates that π-electrons play an important role in defining the main spectral features of benzoheteroles that contain heavier heteroatoms and that the differences in the spectroscopic properties between group 15 and group 16 benzoheteroles are closely associated with their nonplanar or planar geometries. The present theoretical methodology can rationalize the trends observed in the experimental results despite its crude nature. More sophisticated theoretical models including intensities of absorption,[60,61] vibronic effects,[62,63] improved basis sets,[64] relativistic effects,[65,66] and solvent effects[67] as well as simulated MCD spectra[68,69] would help a deeper theoretical analysis. Although the aromaticity of these heterosubstituted compounds would be more complicated than the present simple theoretical model,[70] we believe that the present approach is useful for qualitative understanding of the effect of replacing the heteroatom on the physicochemical properties of other heterocyclic compounds.

Acknowledgment. Calculations were, in part, performed using the RIKEN Super Combined Cluster (RSCC). The authors thank those administering these computational facilities for the generous allocation of computer time. We thank Dr. Andrew E. H. Wheatley (University of Cambridge) for his valuable comments.

Supporting Information Available: Experimental procedures, X-ray crystal analysis, spectral data for group 16 derivatives, and computational details. This material is available free of charge via the Internet at http://pubs.acs.org.

References and Notes

(1) Sundberg, R. J. *Indoles*; Academic Press: San Diego, CA, 1996.
(2) Joule, J. A.; Mills, K.; Smith, G. F. *Heterocyclic Chemistry*, 3rd ed.; Chapman & Hall: New York, 1995.
(3) Hiemstra, H.; Speckamp, W. N. In *The Alkaloids. Chemistry and Pharmacology*; Brossi, A. , Ed.; Academic Press: New York, 1988; Vol. 32, pp 290−307.
(4) Brzozoeski, A. M.; Pike, A. C. W.; Dauter, Z.; Hubbard, R. E.; Bonn, T.; Engström, O.; Öhman, L.; Greene, G. L.; Gustafsson, J.-A.; Carlquist, M. *Nature* **1997**, *389*, 753–758.
(5) Edelhoch, H. *Biochemistry* **1967**, *6*, 1948–1954.
(6) Burstein, E. A.; Vedenkin, N. S.; Ivkova, M. N. *Photochem. Photobiol.* **1973**, *18*, 263–279.
(7) Szabo, A. G.; Rayner, D. M. *J. Am. Chem. Soc.* **1980**, *102*, 554–563.
(8) Creed, D. *Photochem. Photobiol.* **1984**, *39*, 537–562.
(9) Gillam, E. M.; Notley, L. M.; Cai, H.; De Voss, J. J.; Guengerich, F. P. *Biochemistry* **2000**, *39*, 13817–13824.
(10) Anthony, J. E. *Chem. Rev.* **2006**, *106*, 5028–5048.
(11) Ebata, H.; Miyazaki, E.; Yamamoto, T.; Takimiya, K. *Org. Lett.* **2007**, *9*, 4499–4502.
(12) Fukazawa, A.; Hara, M.; Okamoto, T.; Son, E.-C.; Xu, C.; Tamao, K.; Yamaguchi, S. *Org. Lett.* **2008**, *10*, 913–916.
(13) Hamer, F. M. *The Chemistry of Heterocyclic Compound, The Cyanine Dyes and Related Compounds*; Wiley: New York, 1964; Vol *18*.
(14) Fabian, J.; Nakazumi, H.; Matsuoka, M. *Chem. Rev.* **1992**, *92*, 1197–1226.
(15) Mishra, A.; Behera, R. K.; Behera, P. K.; Mishra, B. K.; Behera, G. B. *Chem. Rev.* **2000**, *100*, 1973–2011.
(16) Tian, M.; Tatsuura, S.; Furuki, M.; Sato, Y.; Iwasa, I.; Pu, L. S. *J. Am. Chem. Soc.* **2003**, *125*, 348–349.
(17) Souto, M. A.; Wallace, S. L.; Michl, J. *Tetrahedron* **1980**, *36*, 1521–1530.
(18) Michl, J. *Pure Appl. Chem.* **1980**, *52*, 1549–1563.
(19) Mille, G.; Guilliano, M.; El Jammal, T.; Chouteau, J.; Piette, J.-L. *Spectrochim. Acta* **1983**, *39A*, 1033–1041.
(20) Kurita, J.; Shiratori, S.; Yasuike, S.; Tsuchiya, T. *J. Chem. Soc., Chem. Commun.* **1991**, 1227–1228.
(21) Sashida, H.; Yasuike, S. *J. Heterocycl. Chem.* **1998**, *35*, 725–726.
(22) Takimiya, K.; Kunugi, Y.; Konda, Y.; Ebata, H.; Toyoshima, Y.; Otsubo, T. *J. Am. Chem. Soc.* **2006**, *128*, 3044–3050.
(23) Kurita, J.; Ishii, M.; Yasuike, S.; Tsuchiya, T. *J. Chem. Soc., Chem. Commun.* **1993**, 1309–1310.
(24) Kurita, J.; Ishii, M.; Yasuike, S.; Tsuchiya, T. *Chem. Pharm. Bull.* **1994**, *42*, 1437–1441.
(25) Frisch, M. J.; Trucks, G. W.; Schlegel, H. B.; Scuseria, G. E.; Robb, M. A.; Cheeseman, J. R.; Montgomery, J. A., Jr.; Vreven, T.; Kudin, K. N.;

Burant, J. C.; Millam, J. M.; Iyengar, S. S.; Tomasi, J.; Barone, V.; Mennucci, B.; Cossi, M.; Scalmani, G.; Rega, N.; Petersson, G. A.; Nakatsuji, H.; Hada, M.; Ehara, M.; Toyota, K.; Fukuda, R.; Hasegawa, J.; Ishida, M.; Nakajima, T.; Honda, Y.; Kitao, O.; Nakai, H.; Klene, M.; Li, X.; Knox, J. E.; Hratchian, H. P.; Cross, J. B.; Adamo, C.; Jaramillo, J.; Gomperts, R.; Stratmann, R. E.; Yazyev, O.; Austin, A. J.; Cammi, R.; Pomelli, C.; Ochterski, J. W.; Ayala, P. Y.; Morokuma, K.; Voth, G. A.; Salvador, P.; Dannenberg, J. J.; Zakrzewski, V. G.; Dapprich, S.; Daniels, A. D.; Strain, M. C.; Farkas, O.; Malick, D. K.; Rabuck, A. D.; Raghavachari, K.; Foresman, J. B.; Ortiz, J. V.; Cui, Q.; Baboul, A. G.; Clifford, S.; Cioslowski, J.; Stefanov, B. B.; Liu, G.; Liashenko, A.; Piskorz, P.; Komaromi, I.; Martin, R. L.; Fox, D. J.; Keith, T.; Al-Laham, M. A.; Peng, C. Y.; Nanayakkara, A.; Challacombe, M.; Gill, P. M. W.; Johnson, B.; Chen, W.; Wong, M. W.; Gonzalez, C.; Pople, J. A.; *Gaussian 03*, Revision D.01; Gaussian, Inc.: Wallingford, CT, 2004.

(26) Hay, P. J.; Wadt, W. R. *J. Chem. Phys.* **1985**, *82*, 270–283.

(27) Wadt, W. R.; Hay, P. J. *J. Chem. Phys.* **1985**, *82*, 284–298.

(28) Hay, P. J.; Wadt, W. R. *J. Chem. Phys.* **1985**, *82*, 299–310.

(29) Chang, J. W. W.; Xu, X.; Chan, P. W. H. *Tetrahedron Lett.* **2007**, *48*, 245–248.

(30) Song, P.-S.; Kurtin, W. E. *J. Am. Chem. Soc.* **1969**, *91*, 4892–4906.

(31) Palmer, M. H.; Kennedy, S. M. F. *J. Chem. Soc., Perkin Trans. 2* **1974**, 1893–1903.

(32) Eftink, M. R.; Selvidge, L. A.; Callis, P. R.; Rehms, A. A. *J. Phys. Chem.* **1990**, *94*, 3469–3479.

(33) Westbrook, J. D.; Levy, R. M.; Kroghjespersen, K. *J. Comput. Chem.* **1992**, *13*, 979–989.

(34) Albinsson, B.; Nordén, B. *J. Phys. Chem.* **1992**, *96*, 6204–6212.

(35) Callis, P. R.; Vivian, J. T.; Slater, L. S. *Chem. Phys. Lett.* **1995**, *244*, 53–58.

(36) Serrano-Andres, L.; Roos, B. O. *J. Am. Chem. Soc.* **1996**, *118*, 185–195.

(37) Butkus, E.; Berg, U.; Malinauskienë, J.; Sandström, J. *J. Org. Chem.* **2000**, *65*, 1253–1358.

(38) Platt, J. R. *J. Chem. Phys.* **1949**, *17*, 484–495.

(39) Butler, I. S.; Harrod, H. F. *Inorganic Chemistry, Principles and Applications*; Benjamin Cummings Inc.: Redwood City, CA, 1989.

(40) Decken, A.; Bottomley, F.; Wilkins, B. E.; Grill, E. D. *Organometallics* **2004**, *23*, 3683–3693.

(41) Lee, J.; Liu, Q.-D.; Bai, D.-R.; Kang, Y.; Tao, Y.; Wang, S. *Organometallics* **2004**, *23*, 6205–6213.

(42) van Baar, J. F.; Horton, A. D.; de Kloe, K. P.; Kragtwijk, E.; Mkoyan, S. G.; Nifant'ev, I. E.; Schut, P. A.; Taidakov, I. V. *Organometallics* **2003**, *22*, 2711–2722.

(43) Kurita, J.; Usuda, F.; Yasuike, S.; Tsuchiya, T.; Tsuda, Y.; Kiuchi, F.; Hosoi, S. *Chem. Commun.* **2000**, 191–192.

(44) The P atom in the X ray structure of 1 H-2,3-diphenylphosphindole was reported to be tetrahedrally coordinated. Cordaro, J. G.; Stein, D.; Grützmacher, H. *J. Am. Chem. Soc.* **2006**, *128*, 14962–14971.

(45) Michl, J. *J. Am. Chem. Soc.* **1978**, *100*, 6801–6811.

(46) Michl, J. *J. Am. Chem. Soc.* **1978**, *100*, 6812–6818.

(47) Michl, J. *J. Am. Chem. Soc.* **1978**, *100*, 6819–6823.

(48) Igarashi, N.; Tajiri, A.; Hatano, M. *Bull. Chem. Soc. Jpn.* **1981**, *54*, 1511–1516.

(49) Wallace, S. L.; Michl, J. *Tetrahedron* **1980**, *36*, 1531–1537.

(50) Albinsson, B.; Kubista, M.; Nordén, B.; Thulstrup, E. W. *J. Phys. Chem.* **1989**, *93*, 6646–6654.

(51) Mason, W. R. *A Practical Guide to Magnetic Circular Dichroism Spectroscopy*; John Wiley & Sons Inc.: Hoboken, NJ, 2007.

(52) Nordén, B.; Håkansson, R.; Pedersen, P. B.; Thulstrup, E. W. *Chem. Phys.* **1978**, *33*, 355–366.

(53) Runge, E.; Gross, E. K. U. *Phys. Rev. Lett.* **1984**, *52*, 997–1000.

(54) Bauernschmitt, R. *Ahlrichs Chem. Phys. Lett.* **1996**, *256*, 454–464.

(55) Autschbach, J.; Patchkovskii, S.; Ziegler, T.; van Gisbergen, S. J. A.; Baerends, E. J. *J. Chem. Phys.* **2002**, *117*, 581–592.

(56) Bruice, P. Y. *Organic Chemistry*, 4th ed.; Pearson Education Inc., 2004.

(57) Harder, S.; Boersma, J.; Brandsma, L.; Kanters, J. A.; Bauer, W.; Pi, R.; Schleyer, P. v. R.; Schöllhorn, H.; Thewalt, U. *Organometallics* **1989**, *8*, 1688–1696.

(58) Yamaguchi, T.; Fujita, Y.; Irie, M. *Chem. Commun.* **2004**, 1010–1011.

(59) Rodger, A.; Nordén, B. *Circular Dichroism and Linear Dichroism*; Oxford University Press: Oxford, U.K., 1997.

(60) Miura, M.; Aoki, Y.; Champagne, B. *J. Chem. Phys.* **2007**, *127*, 084103.

(61) Schreiber, M.; Silva-Junior, M. R.; Sauer, S. P. A.; Thiel, W. *J. Chem. Phys.* **2008**, *128*, 134110.

(62) Dierksen, M.; Grimme, S. *J. Phys. Chem. A* **2004**, *108*, 10225–10237.

(63) Guillaume, M.; Liégeois, V.; Champagne, B.; Zutterman, F. *Chem. Phys. Lett.* **2007**, *446*, 165–169.

(64) Check, C. E.; Faust, T. O.; Bailey, J. M.; Wright, B. J.; Gilbert, T. M.; Sunderlin, L. S. *J. Phys. Chem. A* **2001**, *105*, 8111–8116.

(65) van Lenthe, E.; Baerends, E. J.; Snijders, J. G. *J. Chem. Phys.* **1993**, *99*, 4597–4610.

(66) Dyall, K.; van Lenthe, E. *J. Chem. Phys.* **1999**, *111*, 1366–1372.

(67) Klamt, A.; Schüürmann, G. *J. Chem. Soc., Perkin Trans. 2* **1993**, 799–805.

(68) Krykunov, M.; Seth, M.; Ziegler, T. *J. Chem. Phys.* **2007**, *127*, 244102.

(69) Seth, M.; Krykunov, M.; Ziegler, T.; Autschbach, J. *J. Chem. Phys.* **2008**, *128*, 23402.

(70) Soncini, A.; Domene, C.; Engelberts, J. J.; Fowler, P. W.; Rassat, A.; van Lenthe, J. H.; Havenith, R. W. A.; Jenneskens, L. W. *Chem. Eur. J.* **2005**, *11*, 1257–1266.

JP8079843